(Preprint) AAS 17-011

# SPACECRAFT DYNAMICS EMPLOYING A GENERAL MULTI-TANK AND MULTI-THRUSTER MASS DEPLETION FORMULATION

Paolo Panicucci*, Cody Allard† and Hanspeter Schaub‡

Using thrusters for either orbital maneuvers or attitude control change the current spacecraft mass properties and results in an associated reaction force and torque. To perform orbital and attitude control using thrusters, or to obtain optimal trajectories, the impact of mass variation and depletion of the spacecraft must be thoroughly understood. In contrast to earlier works a general solution is developed which makes no assumptions on the body symmetry or tank geometry. The fully coupled translational and rotational equations of motion are derived of a spacecraft that is ejecting mass through the use of thrusters. The formulation considers a general multi-tank and multi-thruster approach to account for both the depleting fuel mass in the tanks and the mass exiting the thruster nozzles. General spacecraft configurations are possible where thrusters can pull from a single tank or multiple tanks, and the tank being drawn from can be switched via a valve. Numerical simulations validate the dynamical model solution and show the impact of assumptions that are made for mass depletion in prior developed models. The results underline the need of implementing a mass depletion model in high-fidelity simulation comparing the developed model with an "Update-Only" model. It results in a difference in the spacecraft's angular velocity between the two models and in a lack of precision in the simpler formulation, the "Update-Only" model.

## INTRODUCTION

The aerospace industry has been steadily increasing the accuracy of spacecraft simulations using advanced analytical development and computer numerical techniques. The prediction of satellite behaviors and their orbits during the preliminary design phase and leading up to the operational period is an extremely useful tool to develop and analyze missions. Moreover, high-fidelity models provide an efficient way to limit fuel demanding maneuvers to preserve satellite orbital position. In this context, the need of a general formulation to predict satellite orbital and attitude behaviors while considering mass depletion is crucial to model the dynamical mass variation influence on the equations of motion (EOMs).

The simplest way to take into account the ejection of propellant is to use an "Update-Only" approach, thus updating the center of mass position and the inertia during the simulation in the EOMs without considering the dynamical influences of the mass depletion. This results in a easy-to-implement model whose limitations consist in the lack of detailed attitude and translational motion prediction for high-fidelity purposes. A more accurate approach considers the spacecraft as an open system whose mass changes in accord with the fuel flows and, consequently, the dynamical variables are transported out of the system using the Reynolds theorem.[1,2] Past works[3,4,5,6] present the derivation of a variable mass rocket with an axial-symmetric design with a single axial-symmetric burn chamber and a circular nozzle. These assumptions decouple the rocket axial spin from the transverse angular velocity and results in a closed solution to the problem. Other works[7,8] present the EOMs considering a system of coaxial bodies with different angular velocities. The studies present an analysis of the nutation angle in the case of a two-body satellite, like a spacecraft with a coaxial wheel. The equations must be specified accordingly with the number of interconnected bodies and

*Graduate Student, Dipartimento di Ingegneria Aerospaziale ed Astronautica, University of Roma "La Sapienza".
†Graduate Student, Aerospace Engineering Sciences, University of Colorado Boulder.
‡Alfred T. and Betty E. Look Professor of Engineering, Department of Aerospace Engineering Sciences, University of Colorado, 431 UCB, Colorado Center for Astrodynamics Research, Boulder, CO 80309-0431. AAS Fellow.

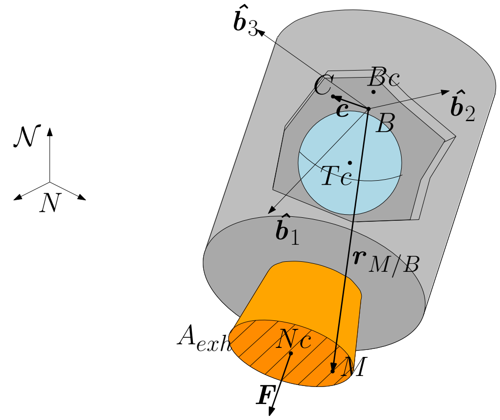


**Figure 1. Spacecraft with depleting mass and definition of frames and variables**

this results in the need of re-derivation for a specific system of interconnected bodies and to take into account how particles leave the system. A more recent work[9] considers a body fixed reference origin and develops the translational and rotational EOM for a reentry module but it lacks in a defined approach to connect the dynamical properties variation with the ejected mass characteristics.

This research is focused on the formalization of a general multi-tank and multi-thruster approach to link the mass depletion inside the tanks with the fuel ejected by the nozzles, and the resulting impact on the orbital and attitude motion. The EOMs are gathered considering a system composed of a general number of tanks and nozzles without making any hypothesis about their properties. Furthermore, the model is thought to be as modular as possible to be easily implemented in flight dynamics software. In the remaining sections, the problem description is outlined, and the fully coupled translational and rotational motion EOMs are developed. Next, the mapping employed from the general multi-tank, multi-thruster model is explained and the mathematical relations are established. Finally, results and conclusion are presented to underline the importance of considering the previously ignored phenomena to obtain close-to-reality simulations and high-accuracy model.

## PROBLEM STATEMENT

To help define the problem, Figure 1 is displayed. This problem involves a spacecraft consisting of a hub which is a rigid body and has a center of mass location labeled as point $B_c$. The hub has $M$ number of tanks and $N$ number of thrusters attached to it. The figure only shows one tank and one thruster but the analytical development is general. The $i_{\text{th}}$ tank has a center of mass location labeled as $Fc_i$ and the $j_{\text{th}}$ thruster is located at $Nc_j$. The body fixed reference frame $\mathcal{B}$: $\{\hat{\boldsymbol{b}}_1, \hat{\boldsymbol{b}}_2, \hat{\boldsymbol{b}}_3\}$ with origin $B$ can be oriented in any direction and point $B$ can be located anywhere fixed to the hub. This means that point $B$ and the center of mass location of the spacecraft, $C$, are not necessarily coincident. As a result, the vector $\boldsymbol{c}$ defines the vector pointing from the body frame origin to the center of mass fo the spacecraft. The inertial reference frame $\mathcal{N}$: $\{\hat{\boldsymbol{n}}_1, \hat{\boldsymbol{n}}_2, \hat{\boldsymbol{n}}_3\}$ is centered at $N$ and is fixed in inertial space.

Throughout this paper, vector calculus is used and the notation to define certain quantities needs to be introduced. A position vector, $\boldsymbol{r}_{C/N}$, is the vector pointing from $N$ to $C$. $\boldsymbol{\omega}_{\mathcal{B}/\mathcal{N}}$ is the angular velocity of the $\mathcal{B}$ frame with respect to the $\mathcal{N}$ frame. $\dot{\boldsymbol{r}}$ denotes an inertial time derivate of vector $\boldsymbol{r}$ and $\boldsymbol{r}'$ defines a time derivate of $\boldsymbol{r}$ with respect to the body frame. Using these definitions, the following describes the Reynolds transport theorem used in this formulation.

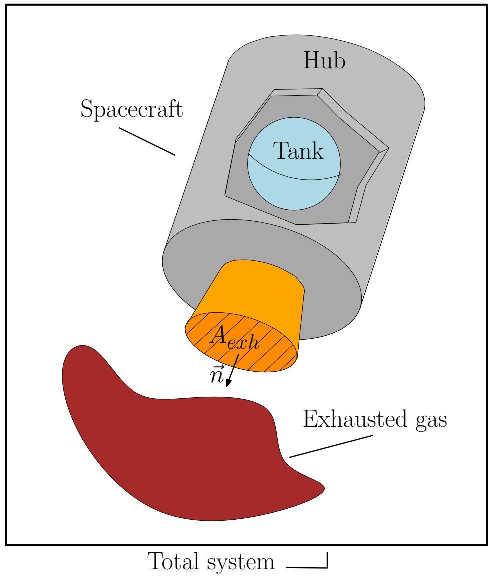


**Figure 2. Division of the total system into the spacecraft and exhausted gas. The control surface $\mathcal{A}_{\text{sc}}$ represents the exchanging surface between the two subsystems.**

## EQUATIONS OF MOTION

### Reynolds Transport Theorem and Continuity Equation

In this section the main tool used for the development of the governing equations is presented and explained. The Reynolds transport theorem provides a basic tool to pass from a Lagrangian formulation, based on the analysis of particles moving in space, to an Eulerian one, which considers a fixed space volume where physical quantities are exchanged through the boundaries.

In the present document, the Lagrangian system is labeled *Body*, the moving volume of the Eulerian approach is labeled $\mathcal{V}_{\text{sc}}$ and its surface $\mathcal{A}_{\text{sc}}$ are represented in Figure 2. By using this notation, the Reynolds transport theorem affirms:[10, 11, 12, 1]

$$\frac{^{\mathcal{D}}\mathrm{d}}{\mathrm{d}t}\int_{\text{Body}} \rho\, \boldsymbol{f} \mathrm{d}\mathcal{V} = \frac{^{\mathcal{D}}\mathrm{d}}{\mathrm{d}\,t}\int_{\mathcal{V}_{\text{sc}}} \rho\, \boldsymbol{f} \mathrm{d}\mathcal{V} + \int_{\mathcal{A}_{\text{sc}}} \rho\, \boldsymbol{f}\left(\boldsymbol{v}_{\text{rel}} \cdot \hat{\boldsymbol{n}}\right) \mathrm{d}A \tag{1}$$

where $\boldsymbol{f}$ is a general vectorial quantity transported out from the control volume, $\rho$ is the density of the infinitesimal mass $\mathrm{d}m$, $\hat{\boldsymbol{n}}$ the surface normal considered positive if exiting from the control volume, $\mathcal{D}$ is a generic reference frame and $\boldsymbol{v}_{\text{rel}}$ is the relative velocity of the particles flowing out from the surface with respect to the control surface itself. This last quantity can be easily defined as

$$\boldsymbol{v}_{\text{rel}}(\boldsymbol{x}, t) = \frac{^{\mathcal{D}}\mathrm{d}}{\mathrm{d}t}\boldsymbol{r}_{M/B}(\boldsymbol{x}, t) - \boldsymbol{v}_{\text{surf}}(\boldsymbol{x}, t) \tag{2}$$

where $\frac{^{\mathcal{D}}\mathrm{d}}{\mathrm{d}t}\boldsymbol{r}_{M/B}(\boldsymbol{x}, t)$ is the particles' velocity with respect to the $\mathcal{D}$ frame and $\boldsymbol{v}_{\text{surf}}(\boldsymbol{x}, t)$ is the control surface velocity with respect to the $\mathcal{D}$ reference frame.

An additional key equation that is used throughout the paper is the continuity equation. First, the continuity equation is gathered:

$$\frac{^{\mathcal{B}}\mathrm{d}}{\mathrm{d}t}\int_{\text{Body}} \rho\, \mathrm{d}m = \frac{^{\mathcal{B}}\mathrm{d}}{\mathrm{d}t}\int_{\mathcal{V}_{\text{sc}}} \rho\, \mathrm{d}\mathcal{V} + \int_{\mathcal{A}_{\text{sc}}} \rho\, \boldsymbol{r}'_{M/B} \cdot \hat{\boldsymbol{n}}\, \mathrm{d}\mathcal{A} = 0 \tag{3}$$

Thus, by defining $\dot{m}_{\text{sc}} = \frac{^{\mathcal{B}}\text{d}}{\text{d}t} \int_{\mathcal{V}_{\text{sc}}} \rho \, \text{d}\mathcal{V}$:

$$\dot{m}_{\text{sc}} = -\int_{\mathcal{A}_{\text{sc}}} \rho \, \boldsymbol{r}'_{M/B} \cdot \hat{\boldsymbol{n}} \, \text{d}\mathcal{A} \qquad \Rightarrow \qquad \text{d}\dot{m} = -\rho \, \boldsymbol{r}'_{M/B} \cdot \hat{\boldsymbol{n}} \, \text{d}\mathcal{A} \tag{4}$$

This definition will be used in the derivation of the EOMs. The translational EOM is developed in the following section.

**Translational Equation of Motion**

The derivation of the translational EOM begins considering Newton's law for a closed system in a non-inertial reference frame:

$$\int_{\text{Body}} \left(\ddot{\boldsymbol{r}}_{B/N} + \dot{\boldsymbol{\omega}}_{\mathcal{B}/\mathcal{N}} \times \boldsymbol{r}_{M/B} + \boldsymbol{\omega}_{\mathcal{B}/\mathcal{N}} \times \left(\boldsymbol{\omega}_{\mathcal{B}/\mathcal{N}} \times \boldsymbol{r}_{M/B}\right)\right) \text{d}m + \\ + 2\,\boldsymbol{\omega}_{\mathcal{B}/\mathcal{N}} \times \int_{\text{Body}} \boldsymbol{r}'_{M/B} \text{d}m + \int_{\text{Body}} \boldsymbol{r}''_{M/B} \text{d}m = \boldsymbol{F}_{\text{ext}} \tag{5}$$

where $\boldsymbol{r}_{M/N}$ is the position of the particle at the $M$ point and $\boldsymbol{F}_{\text{ext}}$ is the sum of the external forces experienced by the body. By using the Reynolds transport theorem, the two previous equations can be expressed in a space fixed volume, shown in Figure 2. Performing this conversion results in the following equations:

$$\frac{^{\mathcal{B}}\text{d}}{\text{d}t} \int_{\text{Body}} \boldsymbol{r}_{M/B} \, \text{d}m = \frac{^{\mathcal{B}}\text{d}}{\text{d}t} \int_{\mathcal{V}_{\text{sc}}} \rho \, \boldsymbol{r}_{M/B} \, \text{d}\mathcal{V} + \int_{\mathcal{A}_{\text{sc}}} \rho \, \boldsymbol{r}'_{M/B} \cdot \hat{\boldsymbol{n}} \, \boldsymbol{r}_{M/B} \text{d}A \tag{6}$$

$$\frac{^{\mathcal{B}}\text{d}^2}{\text{d}t^2} \int_{\text{Body}} \boldsymbol{r}_{M/B} \, \text{d}m = \frac{^{\mathcal{B}}\text{d}^2}{\text{d}t^2} \int_{\mathcal{V}_{\text{sc}}} \rho \, \boldsymbol{r}_{M/B} \, \text{d}\mathcal{V} + \\ + \frac{^{\mathcal{B}}\text{d}}{\text{d}t} \int_{\mathcal{A}_{\text{sc}}} \rho \, \boldsymbol{r}'_{M/B} \cdot \hat{\boldsymbol{n}} \, \boldsymbol{r}_{M/B} \, \text{d}A + \int_{\mathcal{A}_{\text{sc}}} \rho \, \boldsymbol{r}'_{M/B} \cdot \hat{\boldsymbol{n}} \, \boldsymbol{r}'_{M/B} \, \text{d}A \tag{7}$$

where $\boldsymbol{v}_{\text{rel}} = \boldsymbol{r}'_{M/B}$ because point $B$ is fixed with respect to the spacecraft.

As explained in previous work,[10] if all of the mass is contained in the control volume at the initial time, then a particular relation results because no mass is outside the control volume at $t = 0$ and the dynamic quantities will be transported out during the integration. This relationship is quantified in the following equation:

$$\boldsymbol{F}_{\text{ext}} - \int_{\text{Body}} \left(\ddot{\boldsymbol{r}}_{B/N} + \dot{\boldsymbol{\omega}}_{\mathcal{B}/\mathcal{N}} \times \boldsymbol{r}_{M/B} + \boldsymbol{\omega}_{\mathcal{B}/\mathcal{N}} \times \left(\boldsymbol{\omega}_{\mathcal{B}/\mathcal{N}} \times \boldsymbol{r}_{M/B}\right)\right) \text{d}m = \int_{\mathcal{V}_{\text{sc}}} \text{d}\boldsymbol{F}_{\text{vol}} + \\ + \int_{\mathcal{A}_{\text{sc}}} \text{d}\boldsymbol{F}_{\text{surf}} - \int_{\mathcal{V}_{\text{sc}}} \rho \, \left(\ddot{\boldsymbol{r}}_{B/N} + \dot{\boldsymbol{\omega}}_{\mathcal{B}/\mathcal{N}} \times \boldsymbol{r}_{M/B} + \boldsymbol{\omega}_{\mathcal{B}/\mathcal{N}} \times \left(\boldsymbol{\omega}_{\mathcal{B}/\mathcal{N}} \times \boldsymbol{r}_{M/B}\right)\right) \text{d}\mathcal{V} \tag{8}$$

where the forces are divided into volumetric forces and the forces applied on the spacecraft surface. Rearranging this result, replacing the definition of $\boldsymbol{F}_{\text{ext}}$, and isolating the forces to the right hand side of the equation yields:

$$\int_{\mathcal{V}_{\text{sc}}} \rho \, \left(\ddot{\boldsymbol{r}}_{B/N} + \dot{\boldsymbol{\omega}}_{\mathcal{B}/\mathcal{N}} \times \boldsymbol{r}_{M/B} + \boldsymbol{\omega}_{\mathcal{B}/\mathcal{N}} \times \left(\boldsymbol{\omega}_{\mathcal{B}/\mathcal{N}} \times \boldsymbol{r}_{M/B}\right)\right) \text{d}\mathcal{V} + \\ + 2\,\boldsymbol{\omega}_{\mathcal{B}/\mathcal{N}} \times \left( \frac{^{\mathcal{B}}\text{d}}{\text{d}t} \int_{\mathcal{V}_{\text{sc}}} \rho \, \boldsymbol{r}_{M/B} \, \text{d}\mathcal{V} \, + \int_{\mathcal{A}_{\text{sc}}} \rho \, \boldsymbol{r}'_{M/B} \cdot \hat{\boldsymbol{n}} \, \boldsymbol{r}_{M/B} \text{d}A \right) + \frac{^{\mathcal{B}}\text{d}^2}{\text{d}t^2} \int_{\mathcal{V}_{\text{sc}}} \rho \, \boldsymbol{r}_{M/B} \, \text{d}\mathcal{V} + \\ + \frac{^{\mathcal{B}}\text{d}}{\text{d}t} \int_{\mathcal{A}_{\text{sc}}} \rho \, \boldsymbol{r}'_{M/B} \cdot \hat{\boldsymbol{n}} \, \boldsymbol{r}_{M/B} \, \text{d}A + \int_{\mathcal{A}_{\text{sc}}} \rho \, \boldsymbol{r}'_{M/B} \cdot \hat{\boldsymbol{n}} \, \boldsymbol{r}'_{M/B} \, \text{d}A = \int_{\mathcal{V}_{\text{sc}}} \text{d}\boldsymbol{F}_{\text{vol}} + \int_{\mathcal{A}_{\text{sc}}} \text{d}\boldsymbol{F}_{\text{surf}} \tag{9}$$

One goal for this paper is to develop the EOMs of a spacecraft with depleting mass without the necessity of continuing to track the depleted mass once it has left the spacecraft. One aspect of achieving this goal, is to define the center of mass of the spacecraft with respect to point $B$, including the remaining fuel while disregarding the spent fuel. This variable, $\boldsymbol{c} = \boldsymbol{r}_{C/B}$, is defined as:

$$\boldsymbol{c} = \frac{m_{\text{hub}}\, \boldsymbol{r}_{Bc/B} + \sum_{i=1}^{M} m_{\text{fuel}_i}\, \boldsymbol{r}_{Fc_i/B}}{m_{\text{hub}} + \sum_{i=1}^{M} m_{\text{fuel}_i}} \tag{10}$$

where $m_{\text{hub}}$ is the mass of the hub, $m_{\text{fuel}_i}$ is the $i^{\text{th}}$ tank's fuel mass and $\boldsymbol{r}_{Fc_i/B}$ is the position of the center of mass of the $i^{\text{th}}$ tank's. In order to infer the influence of the mass variation in the EOMs the first and second time derivatives with respect to the body frame of $\boldsymbol{c}$ are computed from the definition of $\boldsymbol{c}$.

Using this definition, the translational EOM can be simplified. Additionally, some assumptions need to be defined to further simplify the translational EOM. The hub is assumed to be rigid, therefore deformations are not considered. The mass flow within the tanks and the thrusters is assumed to be a second order effect and ignored for this paper. The particles are assumed to be accelerated instantaneously from the spacecraft velocity, $\dot{\boldsymbol{r}}_{B/N}$, to the exhausted velocity $\boldsymbol{v}_{\text{exh}}$ at the nozzle. And the exhausted velocity $\boldsymbol{v}_{\text{exh}}$ is considered constant and parallel to the nozzle's normal.

The first integral in Eqn. (9) is computed using the fact that $\boldsymbol{r}_{M/B} = \boldsymbol{c} + \boldsymbol{r}_{M/C}$ and the result is shown in the following equation:

$$\begin{aligned}\int_{\mathcal{V}_{\text{sc}}} \rho\, \left(\ddot{\boldsymbol{r}}_{B/N} + \dot{\boldsymbol{\omega}}_{\mathcal{B}/\mathcal{N}} \times \boldsymbol{r}_{M/B} + \boldsymbol{\omega}_{\mathcal{B}/\mathcal{N}} \times \left(\boldsymbol{\omega}_{\mathcal{B}/\mathcal{N}} \times \boldsymbol{r}_{M/B}\right)\right) \mathrm{d}\mathcal{V} = \\ = m_{\text{sc}}\, \ddot{\boldsymbol{r}}_{B/N} + m_{\text{sc}}\, \dot{\boldsymbol{\omega}}_{\mathcal{B}/\mathcal{N}} \times \boldsymbol{c} + m_{\text{sc}}\, \boldsymbol{\omega}_{\mathcal{B}/\mathcal{N}} \times \left(\boldsymbol{\omega}_{\mathcal{B}/\mathcal{N}} \times \boldsymbol{c}\right)\end{aligned} \tag{11}$$

where $m_{\text{sc}} = m_{\text{hub}} + \sum_{i=1}^{M} m_{\text{fuel}_i}$ is the instantaneous mass of the spacecraft. The second and fourth integrals are computed and yield:

$$\frac{{}^{\mathcal{B}}\mathrm{d}}{\mathrm{d}t} \int_{\mathcal{V}_{\text{sc}}} \rho\, \boldsymbol{r}_{M/B}\, \mathrm{d}\mathcal{V} = \frac{{}^{\mathcal{B}}\mathrm{d}}{\mathrm{d}t} \left(m_{\text{sc}}\, \boldsymbol{c}\right) = m_{\text{sc}}\, \boldsymbol{c}' + \dot{m}_{\text{fuel}} \boldsymbol{c} \tag{12}$$

$$\frac{{}^{\mathcal{B}}\mathrm{d}^2}{\mathrm{d}t^2} \int_{\mathcal{V}_{\text{sc}}} \rho\, \boldsymbol{r}_{M/B}\, \mathrm{d}\mathcal{V} = \frac{{}^{\mathcal{B}}\mathrm{d}^2}{\mathrm{d}t^2} \left(m_{\text{sc}}\, \boldsymbol{c}\right) = m_{\text{sc}}\, \boldsymbol{c}'' + 2\, \dot{m}_{\text{fuel}}\, \boldsymbol{c}' + \ddot{m}_{\text{fuel}} \boldsymbol{c} \tag{13}$$

where $\dot{m}_{\text{fuel}} = \sum_{i=1}^{M} \dot{m}_{\text{fuel}_i}$ and $\ddot{m}_{\text{fuel}} = \sum_{i=1}^{M} \ddot{m}_{\text{fuel}_i}$.

In order to find the term calculated on the reference surface seen in the third, fifth and sixth integrals, it is convenient to separate the integrals on the surface of each nozzle. Moreover, as the fuel's properties are flowing out of a surface plane, it is convenient to consider that $\boldsymbol{r}_{M/B} = \boldsymbol{r}_{M/Nc_j} + \boldsymbol{r}_{Nc_j/B}$ where $Nc_j$ is the area's geometric center. Performing these calculations, the integrals result in:

$$\int_{\mathcal{A}_{\text{sc}}} \rho\, \boldsymbol{r}'_{M/B} \cdot \hat{\boldsymbol{n}}\, \boldsymbol{r}_{M/B}\, \mathrm{d}A = -\sum_{j=1}^{N} \int_{\dot{m}_{\text{noz}_j}} \left(\boldsymbol{r}_{M/Nc_j} + \boldsymbol{r}_{Nc_j/B}\right) \mathrm{d}\dot{m} = -\sum_{j=1}^{N} \dot{m}_{\text{noz}_j} \boldsymbol{r}_{Nc_j/B} \tag{14}$$

$$\frac{{}^{\mathcal{B}}\mathrm{d}}{\mathrm{d}t} \int_{\mathcal{A}_{\text{sc}}} \rho\, \boldsymbol{r}'_{M/B} \cdot \hat{\boldsymbol{n}}\, \boldsymbol{r}_{M/B}\, \mathrm{d}A = \frac{{}^{\mathcal{B}}\mathrm{d}}{\mathrm{d}t} \left(-\sum_{j=1}^{N} \dot{m}_{\text{noz}_j} \boldsymbol{r}_{Nc_j/B}\right) = -\sum_{j=1}^{N} \ddot{m}_{\text{noz}_j} \boldsymbol{r}_{Nc_j/B} \tag{15}$$

$$\int_{\mathcal{A}_{\text{sc}}} \rho\, \boldsymbol{r}'_{M/B} \cdot \hat{\boldsymbol{n}}\, \boldsymbol{r}'_{M/B}\, \mathrm{d}A = \sum_{j=1}^{N} \int_{\mathcal{A}_{\text{noz}_j}} \rho\, \boldsymbol{r}'_{M/B} \cdot \boldsymbol{n}\, \boldsymbol{r}'_{M/B} \mathrm{d}A = -\sum_{j=1}^{N} \dot{m}_{\text{noz}_j}\, \boldsymbol{v}_{\text{exh}_j} \tag{16}$$

where $\boldsymbol{v}_{\text{exh}_j}$ is the exhausted velocity of a particle exiting from the $j^{\text{th}}$ nozzle.

The two integrals on the right-hand-side of Eq. (9) depends on the force model chosen. Therefore, to not lose generality, the resulting surface integral due to the pressure jump between the nozzle and the environment is the only term that is analytically computed seen in the following equation:

$$\int_{\mathcal{V}_{sc}} \mathrm{d}\boldsymbol{F}_{\text{vol}} + \int_{\mathcal{A}_{sc}} \mathrm{d}\boldsymbol{F}_{\text{surf}} = \boldsymbol{F}_{\text{ext, vol}} + \boldsymbol{F}_{\text{ext, surf}} + \sum_{j=1}^{N} \frac{\boldsymbol{v}_{\text{exh}_j}}{v_{\text{exh}_j}} A_{\text{noz}_j} \left(p_{\text{exh}_j} - p_{\text{atm}}\right) \tag{17}$$

where $\boldsymbol{F}_{\text{ext, vol}}$ is the sum of the external forces acting on the control volume, $\boldsymbol{F}_{\text{ext, surf}}$ is the sum of the external forces accelerating the control surface, $p_{\text{exh}_j}$ is the particles' exhausted pressure at the $j^{\text{th}}$ nozzle and $p_{\text{atm}}$ is the atmospheric pressure at the flying altitude.

In Eq. (17), the term involving the pressure jump is defined as the well-known thrust force, $\boldsymbol{F}_{\text{thr}_j}$:

$$\boldsymbol{F}_{\text{thr}_j} = \boldsymbol{v}_{\text{exh}_j} \left( \frac{A_{\text{noz}_j}}{v_{\text{exh}_j}} \left(p_{\text{exh}_j} - p_{\text{atm}}\right) + \dot{m}_{\text{noz}_j} \right) = I_{\text{sp}_j}\, g_0\, \dot{m}_{\text{noz}_j} \frac{\boldsymbol{v}_{\text{exh}_j}}{v_{\text{exh}_j}} \tag{18}$$

Finally, Equation (9) is rewritten considering the nozzles' geometry and fluid properties by using Equations (12)-(17). For further simplicity, the cross product is substituted with the associated skew symmetric matrix, and the translational equation is written in a more compact form:

$$\begin{aligned} \ddot{\boldsymbol{r}}_{B/N} + [\tilde{\boldsymbol{c}}]^T \dot{\boldsymbol{\omega}}_{\mathcal{B}/\mathcal{N}} = \frac{\boldsymbol{F}_{\text{thr}}}{m_{\text{sc}}} - 2\,\frac{\dot{m}_{\text{fuel}}}{m_{\text{sc}}} \left(c' + \left[\tilde{\boldsymbol{\omega}}_{\mathcal{B}/\mathcal{N}}\right] \times \boldsymbol{c}\right) - \boldsymbol{c}'' + 2\,\left[\tilde{\boldsymbol{\omega}}_{\mathcal{B}/\mathcal{N}}\right]^T \boldsymbol{c}' + \frac{1}{m_{\text{sc}}} \sum_{j=1}^{N} \ddot{m}_{\text{noz}_j} \boldsymbol{r}_{Fc_j/B} \\ - \ddot{m}_{\text{fuel}}\, \boldsymbol{c} + \left[\tilde{\boldsymbol{\omega}}_{\mathcal{B}/\mathcal{N}}\right]^T \left[\tilde{\boldsymbol{\omega}}_{\mathcal{B}/\mathcal{N}}\right] \boldsymbol{c} + \frac{2}{m_{\text{sc}}} \sum_{j=1}^{N} \dot{m}_{\text{noz}_j} \left[\tilde{\boldsymbol{\omega}}_{\mathcal{B}/\mathcal{N}}\right] \boldsymbol{r}_{Nc_j/B} + \frac{\boldsymbol{F}_{\text{ext, vol}}}{m_{\text{sc}}} + \frac{\boldsymbol{F}_{\text{ext, surf}}}{m_{\text{sc}}} \end{aligned} \tag{19}$$

This EOM is the translational equation for an open system subjected to external forces $\boldsymbol{F}_{\text{ext, vol}}$ and $\boldsymbol{F}_{\text{ext, surf}}$ and thrust $\boldsymbol{F}_{\text{thr}} = \sum_{j=1}^{N} \boldsymbol{F}_{\text{thr}_j}$ due to mass depletion of the spacecraft, represented in Fig. 1. From this equation, it can be deduced that the variation of the mass inside the spacecraft directly impacts the position of the satellite with respect to the origin as the body fixed point $B$ changes its state of motion according to the variation of the tanks' linear inertia. In the next section, the rotational EOM for the spacecraft is developed.

### Rotational Equation of Motion

The goal of this section is to develop the EOM associated with attitude dynamics of a spacecraft with depleting mass due to thrusters pulling mass from fuel tanks. Beginning from the angular momentum equation about point $B$ for a closed system:

$$\int_{Body} \rho\, \boldsymbol{r}_{M/B} \times \ddot{\boldsymbol{r}}_{M/B}\, \mathrm{d}\mathcal{V} + \int_{\text{Body}} \rho\, \boldsymbol{r}_{M/B} \times \ddot{\boldsymbol{r}}_{B/N}\, \mathrm{d}\mathcal{V} = \boldsymbol{L}_B \tag{20}$$

As the mass of the system is constant, the derivative of the angular momentum about point $B$ is inferred from the previously explained Reynold's transport theorem:

$$\int_{Body} \rho\, \boldsymbol{r}_{M/B} \times \ddot{\boldsymbol{r}}_{M/B}\, \mathrm{d}\mathcal{V} = \frac{^{\mathcal{N}}\mathrm{d}}{\mathrm{d}t} \int_{\mathcal{V}_{sc}} \rho\, \boldsymbol{r}_{M/B} \times \dot{\boldsymbol{r}}_{M/B}\, \mathrm{d}\mathcal{V} + \int_{\mathcal{A}_{sc}} \rho\, \boldsymbol{r}'_{M/B} \cdot \hat{\boldsymbol{n}} \left(\boldsymbol{r}_{M/B} \times \dot{\boldsymbol{r}}_{M/B}\right) \mathrm{d}A \tag{21}$$

Moreover, similar to the translational equation, if all the mass of the system is assumed to be contained inside the control volume at the initial time, the following relationship results:

$$\int_{\text{Body}} \rho\, \boldsymbol{r}_{M/B} \times \ddot{\boldsymbol{r}}_{B/N}\, \mathrm{d}\mathcal{V} - \boldsymbol{L}_B = m_{\text{sc}} \boldsymbol{c} \times \ddot{\boldsymbol{r}}_{B/N} - \boldsymbol{L}_{B,\,\text{vol}} - \boldsymbol{L}_{B,\,\text{surf}} \tag{22}$$

where $\boldsymbol{L}_{B,\,\text{vol}}$ and $\boldsymbol{L}_{B,\,\text{surf}}$ are the torques caused by the volume and surface forces about point $B$. The general rotational equation for a control volume in a rotating reference frame is reorganized:

$$\dot{\boldsymbol{H}}_{\text{sc},\,B} + \int_{\mathcal{A}_{sc}} \rho\, \boldsymbol{r}'_{M/B} \cdot \hat{\boldsymbol{n}} \left(\boldsymbol{r}_{M/B} \times \dot{\boldsymbol{r}}_{M/B}\right) \mathrm{d}A + m_{\text{sc}} \boldsymbol{c} \times \ddot{\boldsymbol{r}}_{B/N} = \boldsymbol{L}_{B,\,\text{vol}} + \boldsymbol{L}_{B,\,\text{surf}} \tag{23}$$

To perform the inertial derivative of $\boldsymbol{H}_{\text{sc},\,B}$, first the definition of $\boldsymbol{H}_{\text{sc},\,B}$ is defined:

$$\boldsymbol{H}_{\text{sc},\,B} = [I_{\text{hub},\,B_c}]\,\boldsymbol{\omega}_{\mathcal{B}/\mathcal{N}} + \boldsymbol{r}_{Bc/B} \times m_{\text{hub}}\,\dot{\boldsymbol{r}}_{Bc/B} + \\ + \sum_{i=1}^{M}\left([I_{\text{fuel}_i,\,Fc_i}]\;\boldsymbol{\omega}_{\mathcal{B}/\mathcal{N}} + \boldsymbol{r}_{Fc_i/B} \times m_{\text{fuel}_i}\,\dot{\boldsymbol{r}}_{Fc_i/B}\right) \quad (24)$$

where $[I_{\text{hub},\,B_c}]$ is the hub's inertia about its center of mass, $B_c$, and $[I_{\text{fuel}_i,\,Fc_i}]$ is the $i^{\text{th}}$ tank's inertia about its center of mass, $Fc_i$.

Furthermore, by noticing that the inertial time derivatives of the vectors $\boldsymbol{r}_{Bc/B}$ and $\boldsymbol{r}_{Fc_i/B}$ are computed using the transport theorem between the two reference frames and, considering that the point $B_c$ is fixed in the $\mathcal{B}$ frame, an analytical expression of mass depletion in the rotational motion is deduced:

$$\dot{\boldsymbol{H}}_{\text{sc},\,B} = [I_{\text{hub},\,Bc}]\,\dot{\boldsymbol{\omega}}_{\mathcal{B}/\mathcal{N}} + \boldsymbol{\omega}_{\mathcal{B}/\mathcal{N}} \times \left([I_{\text{hub},\,Bc}]\,\boldsymbol{\omega}_{\mathcal{B}/\mathcal{N}}\right) + \boldsymbol{r}_{Bc/B} \times m_{\text{hub}}\,\left(\dot{\boldsymbol{\omega}}_{\mathcal{B}/\mathcal{N}} \times \boldsymbol{r}_{Bc/B} + \right. \\ \left. + \,\boldsymbol{\omega}_{\mathcal{B}/\mathcal{N}} \times \left(\boldsymbol{\omega}_{\mathcal{B}/\mathcal{N}} \times \boldsymbol{r}_{Bc/B}\right)\right) + \sum_{i=1}^{M}\Big([I_{\text{fuel}_i,\,Fc_i}]\,\dot{\boldsymbol{\omega}}_{\mathcal{B}/\mathcal{N}} + \boldsymbol{\omega}_{\mathcal{B}/\mathcal{N}} \times \left([I_{\text{fuel}_i,\,Fc_i}]\,\boldsymbol{\omega}_{\mathcal{B}/\mathcal{N}}\right) + \\ + \boldsymbol{r}_{Fc_i/B} \times m_{\text{fuel}_i}\left(\boldsymbol{r}''_{Fc_i/B} + 2\,\boldsymbol{\omega}_{\mathcal{B}/\mathcal{N}} \times \boldsymbol{r}'_{Fc_i/B} + \dot{\boldsymbol{\omega}}_{\mathcal{B}/\mathcal{N}} \times \boldsymbol{r}_{Fc_i/B} + \boldsymbol{\omega}_{\mathcal{B}/\mathcal{N}} \times \left(\boldsymbol{\omega}_{\mathcal{B}/\mathcal{N}} \times \boldsymbol{r}_{Fc_i/B}\right)\right) + \\ + \boldsymbol{r}_{Fc_i/B} \times \dot{m}_{\text{fuel}_i}\,\left(\boldsymbol{r}'_{Fc_i/B} + \boldsymbol{\omega}_{\mathcal{B}/\mathcal{N}} \times \boldsymbol{r}_{Fc_i/B}\right) + [I_{\text{fuel},_i,\,Fc_i}]'\;\boldsymbol{\omega}_{\mathcal{B}/\mathcal{N}}\Big) \quad (25)$$

It should be noted here that any relative motion of particles inside the fuel tanks of the spacecraft is neglected and, as a consequence, the effects both of the Coriolis' acceleration and of the whirling motion of the fuel on the spacecraft dynamics have not been considered. A more detailed explanation of the impact of these effects can be found in Reference.[6]

In order to simplify Eq. (25) the following inertia matrices are defined using the skew symmetric matrix to replace the cross product:

$$[I_{\text{hub},\,B}] = [I_{\text{hub},\,Bc}] + m_{\text{hub}}\,\left[\tilde{\boldsymbol{r}}_{Bc/B}\right]\left[\tilde{\boldsymbol{r}}_{Bc/B}\right]^T \quad (26)$$

$$[I_{\text{fuel}_i,\,B}] = [I_{\text{fuel}_i,\,Fc_i}] + m_{\text{fuel}_i}\,\left[\tilde{\boldsymbol{r}}_{Fc_i/B}\right]\left[\tilde{\boldsymbol{r}}_{Fc_i/B}\right]^T \quad (27)$$

$$[I_{\text{sc},\,B}] = [I_{\text{hub},\,B}] + \sum_{i=1}^{M}[I_{\text{fuel}_i,\,B}] \quad (28)$$

Moreover, using the Jacobi identity for the cross product, $\mathbf{a} \times (\mathbf{b} \times \mathbf{c}) + \mathbf{b} \times (\mathbf{c} \times \mathbf{a}) + \mathbf{c} \times (\mathbf{a} \times \mathbf{b}) = \mathbf{0}$, the body relative time derivative of the fuel inertia in the $\mathcal{B}$ reference frame is introduced:

$$\boldsymbol{r}_{Fc_i/B} \times \left(2\,\boldsymbol{\omega}_{\mathcal{B}/\mathcal{N}} \times \boldsymbol{r}'_{Fc_i/B}\right) = -\,\boldsymbol{r}_{Fc_i/B} \times \left(\boldsymbol{r}'_{Fc_i/B} \times \boldsymbol{\omega}_{\mathcal{B}/\mathcal{N}}\right) + \\ -\,\boldsymbol{r}'_{Fc_i/B} \times \left(\boldsymbol{r}_{Fc_i/B} \times \boldsymbol{\omega}_{\mathcal{B}/\mathcal{N}}\right) + \boldsymbol{\omega}_{\mathcal{B}/\mathcal{N}} \times \left(\boldsymbol{r}_{Fc_i/B} \times \boldsymbol{r}'_{Fc_i/B}\right) \quad (29)$$

$$[I_{\text{fuel}_i,\,B}]' = [I_{\text{fuel}_i,\,Fc_i}] + \dot{m}_{\text{fuel}_i}\,\left[\tilde{\boldsymbol{r}}_{Fc_i/B}\right]\left[\tilde{\boldsymbol{r}}_{Fc_i/B}\right]^T \\ + m_{\text{fuel}_i}\,\left(\left[\tilde{\boldsymbol{r}}_{Fc_i/B}\right]\left[\tilde{\boldsymbol{r}}'_{Fc_i/B}\right]^T + \left[\tilde{\boldsymbol{r}}'_{Fc_i/B}\right]\left[\tilde{\boldsymbol{r}}_{Fc_i/B}\right]^T\right) \quad (30)$$

Considering that at the nozzles's exit, $\dot{\boldsymbol{r}}_{M/B} = \boldsymbol{v}_{exh_j} + \boldsymbol{\omega}_{\mathcal{B}/\mathcal{N}} \times \boldsymbol{r}_{M/B}$ and $\mathrm{d}\dot{m} = -\rho\,\boldsymbol{r}'_{M/B} \cdot \hat{\boldsymbol{n}}\,\mathrm{d}A$, the surface integral is expressed in terms of the nozzles' surface:

$$\int_{A_{\text{exh}}} \rho\,\boldsymbol{r}'_{M/B} \cdot \boldsymbol{n}\left(\boldsymbol{r}_{M/B} \times \dot{\boldsymbol{r}}_{M/B}\right)\mathrm{d}A = -\sum_{j=1}^{N}\int_{\dot{m}_{\text{noz}_j}} \boldsymbol{r}_{M/B} \times \boldsymbol{v}_{\text{exh}_j}\,\mathrm{d}\dot{m} + \\ + \sum_{j=1}^{N}\int_{\dot{m}_{\text{noz}_j}} \boldsymbol{r}_{M/B} \times \left(\boldsymbol{r}_{M/B} \times \boldsymbol{\omega}_{\mathcal{B}/\mathcal{N}}\right)\,\mathrm{d}\dot{m} \quad (31)$$

The torque of each thruster nozzle is computed by the exhausting flow pressure distribution and by the lever arm distance from point $B$ and the application point of the force:

$$\boldsymbol{L}_{B_{\text{thr}_j}} = \boldsymbol{L}_{B_{\text{sc, noz}_j}} + \int_{\dot{m}_{\text{noz}_j}} \boldsymbol{r}_{M/B} \times \boldsymbol{v}_{\text{noz}_j}\, \mathrm{d}\dot{m} \tag{32}$$

Furthermore, a term taking into account the angular momentum variation caused by mass depletion is defined:

$$[K] = \sum_{i=1}^{M} [I_{\text{fuel}_i,\, B}]' + \sum_{j=1}^{N} \int_{\dot{m}_{\text{noz}_j}} [\tilde{\boldsymbol{r}}_{M/B}]\, [\tilde{\boldsymbol{r}}_{M/B}]\, \mathrm{d}\dot{m} \tag{33}$$

The integral in Eq. (33) is computed evaluating the momentum exchanged due to the fuel exiting a circular nozzle area, coincident with the interface surface between the spacecraft and the exhausted fuel:

$$\int_{\dot{m}_{\text{noz}_j}} [\tilde{\boldsymbol{r}}_{M/B}]\, [\tilde{\boldsymbol{r}}_{M/B}]\, \mathrm{d}\dot{m} = -\dot{m}_{\text{noz}_j} \left( [\tilde{\boldsymbol{r}}_{Nc_j/B}]\, [\tilde{\boldsymbol{r}}_{Nc_j/B}]^T + \frac{A_{\text{noz}_j}}{4\,\pi} [BM_j] \begin{bmatrix} 2 & 0 & 0 \\ 0 & 1 & 0 \\ 0 & 0 & 1 \end{bmatrix} [BM_j]^T \right) \tag{34}$$

where $A_{\text{noz}_j}$ is the exiting area of the $j^{\text{th}}$ nozzle and $[BM_j]$ is the direction cosine matrix (DCM) from the $j^{\text{th}}$ nozzle frame $\mathcal{M}_j$, defined to have its origin at the $Nc_j$ point and its first axis in the exhausting velocity direction $\boldsymbol{v}_{\text{exh}_j}$, to the $\mathcal{B}$ frame. Finally the rotational EOM in Eqn. (23) is written using Equations (24)-(34):

$$\begin{aligned}
[I_{\text{sc},\,B}]\, \dot{\boldsymbol{\omega}}_{\mathcal{B}/\mathcal{N}} + m_{\text{sc}}\, [\tilde{\boldsymbol{c}}]\, \ddot{\boldsymbol{r}}_{B/N} = {} & [\tilde{\boldsymbol{\omega}}_{\mathcal{B}/\mathcal{N}}]^T\, [I_{\text{sc},\,B}]\, \boldsymbol{\omega}_{\mathcal{B}/\mathcal{N}} - [K]\, \boldsymbol{\omega}_{\mathcal{B}/\mathcal{N}} + \\
& + \sum_{i=1}^{M} \Big( m_{\text{fuel}_i}\, [\tilde{\boldsymbol{r}}_{Fc_i/B}]^T\, \boldsymbol{r}''_{Fc_i/B} + m_{\text{fuel}_i}\, [\tilde{\boldsymbol{\omega}}_{\mathcal{B}/\mathcal{N}}]^T\, [\tilde{\boldsymbol{r}}_{Fc_i/B}]\, \boldsymbol{r}'_{Fc_i/B} + \\
& + \dot{m}_{\text{fuel}_i}\, [\tilde{\boldsymbol{r}}_{Fc_i/B}]^T\, \boldsymbol{r}'_{Fc_i/B} \Big) + \boldsymbol{L}_{B,\,\text{vol}} + \boldsymbol{L}_{B,\,\text{surf}} + \sum_{j=1}^{N} \boldsymbol{L}_{B_{\text{thr}_j}}
\end{aligned} \tag{35}$$

This concludes the derivation of the EOMs needed to describe the translational and rotational motion of a spacecraft with depleting mass due to thrusters. The following section describes a method used to implement the relationship between thrusters and fuel tanks.

## FUEL SUPPLY ARCHITECTURE AND IMPLEMENTATION

From a simulation implementation prospective, the tank mass flow rates and their associated derivatives must be computed to evaluate the different terms in the EOMs. This approach assumes that the $j^{\text{th}}$ nozzle mass flow is a known quantity and is computed using Eq. (18) and then the tanks' mass variation $\dot{m}_{\text{fuel}_i}$ is computed. The $i^{\text{th}}$ tank's mass variation is expressed as a linear combination of the fuel ejected by the nozzle where the coefficient, $A_{ij}$, linking the $i^{\text{th}}$ tank with the $j^{\text{th}}$ nozzle is the ratio of the mass released by the tank flowing to that nozzle to the total mass released by that tank.

$$\dot{m}_{\text{fuel}_i} = \sum_{j=1}^{N} A_{ij}\, \dot{m}_{\text{noz}_j} \qquad \Rightarrow \qquad \dot{\boldsymbol{m}}_{\text{fuel}} = [A]\, \dot{\boldsymbol{m}}_{\text{noz}} \tag{36}$$

where $[A]$ is a matrix linking the tanks' and nozzles' mass flow rates. A fundamental property of the matrix $[A]$ is established from the definition of $\dot{m}_{\text{fuel}}$:

$$\sum_{i=1}^{M} \dot{m}_{\text{fuel}_i} = \sum_{i=1}^{M} \sum_{j=1}^{N} A_{ij} \dot{m}_{\text{noz}_j} = \sum_{j=1}^{N} \dot{m}_{\text{noz}_j} \quad \Rightarrow \quad \sum_{i=0}^{M} A_{ij} = 1 \quad \forall j \in (1, N) \tag{37}$$

The previous relation is a direct consequence of the mass flow conservation between the tanks and the nozzles. From the previous relation, the first derivative of mass flows is computed:

$$\ddot{\boldsymbol{m}}_{\text{fuel}} = [A]\, \ddot{\boldsymbol{m}}_{\text{noz}} + [\dot{A}] \dot{\boldsymbol{m}}_{\text{noz}} \tag{38}$$

## CONTROL FEEDBACK LAW

In order to give a meaningful example using the EOMs developed, a control law is introduced in this section for which the simulation results included in the next section utilize.

A Modified Rodrigues Parameters (MRP) feedback control law is chosen as it can always assure global asymptotic stability avoiding singularities and using certain assumptions.[13] If a reference frame $\mathcal{R}$ is defined, the control is expressed as follows:

$$\boldsymbol{u} = -K\,\boldsymbol{\sigma}_{\mathcal{B}/\mathcal{R}} - P\,\boldsymbol{\omega}_{\mathcal{B}/\mathcal{R}} \tag{39}$$

where $\boldsymbol{\sigma}_{\mathcal{B}/\mathcal{R}}$ is the MRP defining the attitude of $\mathcal{B}$ with respect to $\mathcal{R}$ and $\boldsymbol{\omega}_{\mathcal{B}/\mathcal{R}}$ is the angular velocity of $\mathcal{B}$ with respect to $\mathcal{R}$. Moreover, to avoid singularities of the MRP set $\boldsymbol{\sigma}_{\mathcal{B}/\mathcal{R}}$, the MRP can be switched to the shadow set representation.[13]

The control torque can be applied to the spacecraft through various devices, but in the present work a thruster-based control is implemented to underline the main features of mass depletion. The results from simulations are included in the following section.

## RESULTS

This section provides simulations to both validate the EOMs developed and to show the impact of mass depletion on a specific scenario. In the first example, a simulation is developed to compare results to prior developed models. Following this, an example is included that involves a fuel demanding maneuver that highlights the importance of considering mass depletion for high-accuracy pointing, simulation and control law design.

### Validating simulations: Axial-symmetric Rocket

The following simulations are performed to reproduce the results outlined in Reference.[3] The spacecraft under study is an axial-symmetric rocket represented in Figure 3 where the geometrical features of the rocket are shown. The numerical values used in the simulations are chosen accordingly with the NASA publication.[3]

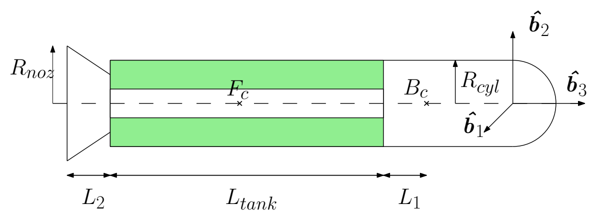


**Figure 3. Geometrical properties of the axial-symmetrical rocket**

In the publication, dimensionless variables are used and their primitive definitions can be found using the following formulas:

$$\beta = \frac{R_{\text{noz}}}{R_{\text{cyl}}} \quad \delta_{1,2} = \frac{L_{1,2}}{R_{\text{cyl}}} \quad \delta = \frac{L}{R_{\text{cyl}}} \quad \psi = \frac{m_{\text{hub}}}{m_{\text{fuel}_0}} \quad \gamma_1 = \frac{k_{\text{hub}_{12}}}{R_{\text{cyl}}} \quad \gamma_2 = \frac{k_{\text{hub}_3}}{R_{\text{cyl}}} \quad \alpha = \frac{\dot{m}_{\text{fuel}}}{m_{\text{fuel}_0}} \tag{40}$$

where $k_{\text{hub}_{12}}$ is the hub's gyration radius of the $\hat{\boldsymbol{b}}_1$ or the $\hat{\boldsymbol{b}}_2$ about the $B_c$ point and $k_{\text{hub}_3}$ is the hub's gyration radius of the $\hat{\boldsymbol{b}}_3$ about the same point. The numerical dimensionless coefficients' values are reported in Table 1. The spin rate, $\omega_{\mathcal{B}/\mathcal{N}_z} = \boldsymbol{\omega}_{\mathcal{B}/\mathcal{N}} \cdot \hat{\boldsymbol{b}}_3$, is presented for the two tank's cases given in Reference.[3] Figure 4 shows that the behavior of the angular velocity for the entirety of the simulation match the previous work from Reference.[3] These results give validation of the model developed in this work. It is important to point out, however, that the model presented in this paper does not constrain the analysis to axial-symmetric bodies. It is developed in a general way that can apply to many spacecraft configurations.

**Table 1. Dimensionless parameters for the axial-symmetrical rocket simulation**

| $\delta_1$ | $\delta_2$ | $\gamma_1$ | $\gamma_2$ | $\alpha$ | $\delta$ | $\psi$ |
|---|---|---|---|---|---|---|
| 2 | 3 | 1.2 | 1 | 0.01 | 10 | 2 |

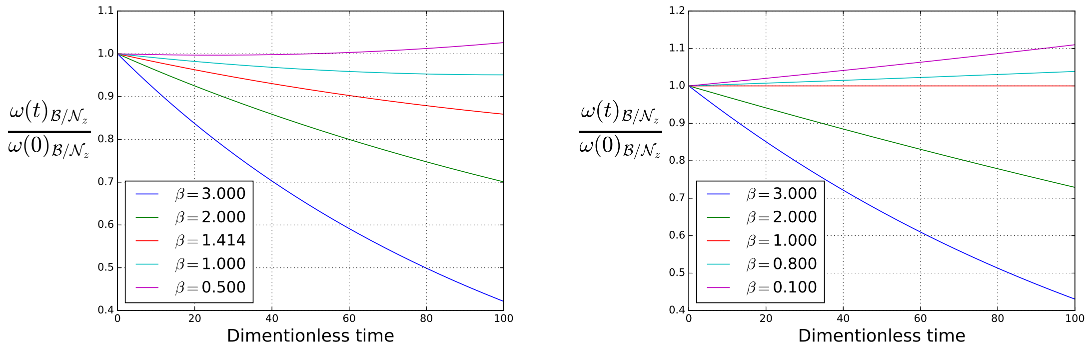


(a) Cetrifugal burn tank

(b) Unifrom cylinder tank

**Figure 4. Spinning rate $\omega_{\mathcal{B}/\mathcal{N}_z}$ evolution in time.**

**On-orbit spacecraft simulations : LEO-to-GEO Transfer**

In this section a geostationary transfer maneuver from LEO (Low Earth Orbit) to GEO (Geostationary Earth Orbit) using a Hohmann transfer maneuver is implemented. To highlight the impacts of mass depletion, a two-body-problem gravity field is considered and no gravity torque perturbation is included.

In this scenario, the satellite has a 12-ADC nozzle cluster in a symmetric configuration to control the attitude of the spacecraft and it is equipped with two delta-velocity (DV) thrusters to perform the firing at apogee and at perigee of the elliptic orbit. The geometrical features are presented in Table 2.

Three scenarios are simulated for this example to highlight the impact of mass depletion on the dynamics of the spacecraft. An "Update-Only" simulation is the first scenario considered and is very commonly used in industry. This involves only updating the current mass properties of the spacecraft but not considering the influence of mass depletion on the system. Additionally, there is not a control law on the attitude of the spacecraft implemented in this scenario. In contrast, the second scenario is named "No-Control" and is a scenario in which the attitude of the satellite is not being controlled, however, this scenario does use the full dynamical model developed in this paper. Lastly, the "Active-Control" scenario considers the developed model along with the previously introduced attitude control law.

The initial conditions along with assumptions being made will constrict the satellite to only rotate about the $\hat{\boldsymbol{b}}_1$ axis. Therefore, the numerical results between the "Update-Only" and the "No-Control" scenarios

| $m_{\text{hub}}$ $[kg]$ | $I_{\text{hub}, Bc_{11}}$ $[kg\, m^2]$ | $I_{\text{hub}, Bc_{22}}$ $[kg\, m^2]$ | $I_{\text{hub}, Bc_{33}}$ $[kg\, m^2]$ |
|---|---|---|---|
| 750.0 | 900.0 | 800.0 | 600.0 |

| $I_{\text{sp}_j}$ $[s]$ $\forall j \in [1,\ 14]$ | $m_{\text{tank}_i}$ $[kg]$ $\forall i \in [1,\ 2]$ | $A_{\text{noz}_j}$ $[m^2]$ $\forall j \in [3,\ 14]$ | $A_{\text{noz}_j}$ $[m^2]$ $\forall j \in [1,\ 2]$ | $R_{\text{tank}_i}$ $[m]$ $\forall i \in [1,\ 2]$ |
|---|---|---|---|---|
| 300.0 | 1060.0 | 0.07 | 0.2 | 0.5 |

**Table 2. Geometrical characteristics of the satellite for the Hohmann transfer.**

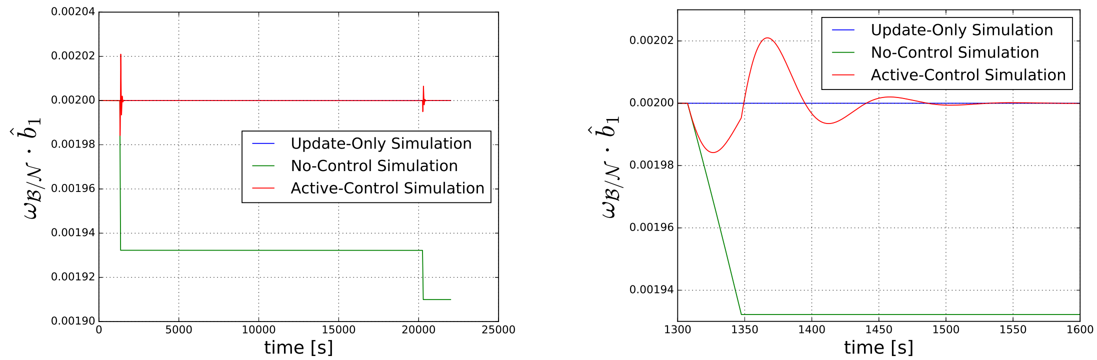


(a) General behavior for the coplete simuation.

(b) Details for the first firing period.

**Figure 5. Projection of $\omega_{\mathcal{B}/\mathcal{N}}$ on the $\hat{b}_3$ axis.**

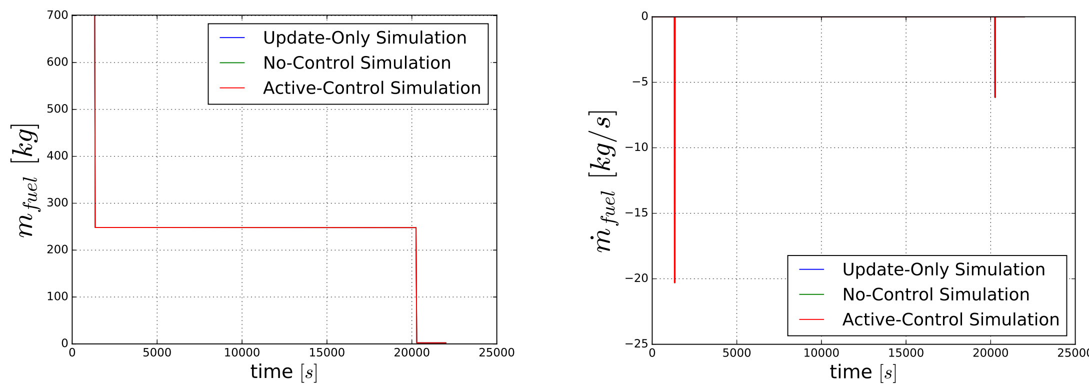


(a) $m_{\text{fuel}}$

(b) $\dot{m}_{\text{fuel}}$

**Figure 6. Mass variation during the Hohmann maneuver simulation.**

will directly show the impact of mass depletion on the dynamics of the satellite. The numerical results of the simulation are presented in Figures 5 and 6.

In Fig. 5(a), the complete 6 hr simulation is presented to compare the previously listed simulations. By comparing the Update-Only scenario with the No-Control scenario, there is a noticeable difference in the angular velocity of the system which is caused by the dynamical effects introduced by the mass depletion. The fact that the angular velocity variation in the No-Control case is negative along with the magnitude of the angular velocity variation are due to the DV thrusters' configuration, both in term of position and geometry, and the tanks' location and dimension as seen in Eq. (33). Obviously changing the properties of either one of the two features will lead to a different solution in terms of amplitude and sign. The results show that the Update-Only scenario does not show any change to the angular velocity due to mass depletion, while the No-Control case does. This difference can lead to a dramatic differences in results and gives importance to the model developed in this paper. In this particular case, the error introduced by mass depletion is about $4\,\%$.

In Figure 5(a), a portion of the first DV burn is displayed to get a better view of the transient. This result is important because it highlights the difference between the Update-Only and the Active-Control scenarios. As discussed previously, this shows that the Update-Only approach indicates no change in the angular velocity. However, with the dynamics developed in this paper, to keep the spacecraft with the desired angular velocity, the Active-Control shows that control is required and the the transient due to the ACS thrusters controlling the spacecraft can be seen in Fig. 5(a).

## CONCLUSIONS

A review of the previous work on the dynamics of spacecraft with mass depletion due to thrusters shows that the rocket-geometry inspired assumptions being made limit the applicability of the dynamics models to many spacecraft. This work develops the translational and rotational EOMs while keeping the formulation as general as possible. This results in arriving at a complete solution that gets rid of the need to rederive the EOMs for specific spacecraft. A novel and compact form of the EOMs is introduced in the case of a realistic multi-tank and multi-thruster configuration that provides rapid and efficient formulation to perform simulations. Additionally, the general derivation allows the model to be expanded quite easily to include effects like panels' deployment or flexible structures, without loss of generality.

The model is validated by comparing a simulation to prior models on mass depletion. The importance of considering mass depletion is proven by comparing the full model developed in this paper with a solution where the mass properties of the spacecraft are just updated each time step. This gives an error of $4\,\%$ on the spacecraft angular velocity with the chosen geometrical features. Depending on the scenario, this error could be much worse and highlights the main desire to consider mass depletion using this model. Ignoring these effects of mass depletion could lead to hastened de-saturation maneuvers or cause inaccurate pointing and unpredicted errors in orientation and position of the spacecraft.

Some limiting assumptions are introduced to this model that do not allow the EOMs to consider the effect of whirling motions or relative fuel motion in the distribution of the system. Future works could consider the influence of whirling motion using a simple formulation or introduction of reaction wheels to simulate complex de-saturation maneuvers.

## ACKNOWLEDGMENT

This work was supported by the Italian Space Agency (ASI) in collaboration with the Cultural Association of Italians at Fermilab (CAIF).

## REFERENCES

[1] J. F. Thorpe, "On the momentum theorem for a continuous system of variable mass," *Am. J. Phys*, Vol. 30, 1962, pp. 637–640.

[2] C. Grubin, "Mechanics of variable mass systems," *Journal of the Franklin Institute*, Vol. 276, No. 4, 1963, pp. 305–312.

[3] F. O. Eke, "Dynamics of variable mass systems," 1998.

[4] F. Eke, T. Tran, and J. Sookgaew, "Dynamics of a Spinning Rocket with Internal Mass Flow," *Nonlinear Dynamics and Systems Theory*, Vol. 6, No. 2, 2006, pp. 129–142.

[5] J. Sookgaew and F. Eke, "Effects of substantial mass loss on the attitude motions of a rocket-type variable mass system," *Nonlinear Dynamics and Systems Theory*, Vol. 4, No. 1, 2004, pp. 73–88.

[6] M. I. Marmureanu and I. Fuiorea, "Attitude Dynamics of a Spinning Rocket with Internal Fluid Whirling Motion," *INCAS Bulletin*, Vol. 6, No. 2, 2014, p. 75.

[7] V. Aslanov and A. Doroshin, "The motion of a system of coaxial bodies of variable mass," *Journal of Applied Mathematics and Mechanics*, Vol. 68, No. 6, 2004, pp. 899–908.

[8] A. V. Doroshin, "Analysis of attitude motion evolutions of variable mass gyrostats and coaxial rigid bodies system," *International Journal of Non-Linear Mechanics*, Vol. 45, No. 2, 2010, pp. 193–205.

[9] M. B. Quadrelli, J. Cameron, B. Balaram, M. Baranwal, and A. Bruno, "Modeling and Simulation of Flight Dynamics of Variable Mass Systems," 2014.

[10] R. W. Fox, A. T. McDonald, and P. J. Pritchard, *Introduction to fluid mechanics*, Vol. 7. John Wiley & Sons New York, 1985.

[11] F. White, *Fluid Mechanics*. McGraw-Hill series in mechanical engineering, McGraw Hill, 2011.

[12] B. Munson, A. Rothmayer, and T. Okiishi, *Fundamentals of Fluid Mechanics, 7th Edition*. John Wiley & Sons, Incorporated, 2012.

[13] H. Schaub and J. L. Junkins, *Analytical Mechanics of Space Systems*. Reston, VA: AIAA Education Series, 3rd ed., 2014, 10.2514/4.102400.